Characterization of phases and determination of phase relations in the Cu-In-S system by γ-γ perturbed angular correlations

H. Metzner
Bereich Schwerionenphysik, Hahn-Meitner-Institut, 1000 Berlin 39, Federal Republic of Germany and Fachbereich Physik, Freie Universität, 1000 Berlin 33, Federal Republic of Germany

M. Brüssler
Bereich Schwerionenphysik, Hahn-Meitner-Institut, 1000 Berlin 39, Federal Republic of Germany

K.-D. Husemann and H. J. Lewerenz
Bereich Photochemische Energieumwandlung, Hahn-Meitner-Institut, 1000 Berlin 39, Federal Republic of Germany
(Received 14 May 1991)

Perturbed angular correlations (PAC's) of γ rays are applied to phase identification and determination of phase relations in the Cu-In-S system at room temperature. Using metallic indium, containing radioactive ^{111}In-^{111}Cd tracers, as starting material, various single and multiphase samples of chosen compositions were grown from the melt and characterized by PAC's. Thus, we identified three Cu-In phases, the In-S phase In_6S_7, and the ternary phases $CuIn_5S_8$ and $CuInS_2$ by means of their PAC signals. When combined with the already known PAC parameters of $CuIn_2$, In, InS, and In_2S_3, these data constitute a complete description of all room-temperature phases of the Cu-In-S system which contain In. PAC measurements of the multiphase samples show that no further In phases exist and allow the determination of several equilibrium lines in the Gibbs phase triangle. Consequences for the crystal growth of $CuInS_2$ are discussed.

I. INTRODUCTION

The ternary chalcopyrite $CuInS_2$ is a promising candidate for applications in thin-film solar cells.[1] Due to its energy gap of $E_g = 1.5$ eV it should in principle be better suited for this purpose than the analogous $CuInSe_2$ compound ($E_g = 1.0$ eV). However, a conversion efficiency of 12% for a $CuInSe_2$ based solar cell has already been reported in 1975,[2] whereas the values for $CuInS_2$ eevices have not to date exceeded 9.7%.[3] A conversion efficiency of 7.3% was recently demonstrated for a thin-film solar cell using $CuInS_2$ as an absorber material.[4]

We have described an electrochemical solar cell based on polycrystalline n-type $CuInS_2$ bulk material which yielded 9.7% conversion efficiency.[3] The comparatively good quality of that material was attributed to spherical In precipitates acting as impurity gettering centers.[5] The polycrystalline $CuInS_2$ material in the thin films produced by Mitchell, Pollock, and Mason contained In_2S_3 and $Cu_{2-x}S$ as minor phases.[4] These examples show that investigations outside the homogeneity range of the $CuInS_2$ compound are essential for a detailed understanding of this material and for its development.

In a preceding paper, we have demonstrated that the observation of perturbed angular correlations (PAC's) of γ rays using ^{111}In-^{111}Cd nuclear probes is a well-suited method to serve the above mentioned purpose.[6] In the case of stoichiometric $CuInS_2$, we found perfect cubic symmetry for the normal In site. Hence, in contrast to literature data,[7] our results gave no indication of a tetragonal distortion of the $CuInS_2$ unit cell. A sample prepared from stoichiometric $CuInS_2$ and metallic In, with excess sulfur in the gas phase, revealed the PAC signals of metallic In, InS, and a cubic fraction due to $CuInS_2$. The coexistence of these three phases in thermal equilibrium allowed us to draw a new tie line in the Gibbs phase triangle which connects $CuInS_2$ and InS. Samples with compositions corresponding to points on that line were produced and their PAC spectra analyzed.

The PAC method allows the determination of the electric-field-gradient (EFG) tensors acting at the sites of an ensemble of typically 10^{10} probe nuclei.[8] The EFG reflects details of the local charge distribution at the probe's site which in turn depends on the local structure including structural and electronic perturbations.[9] In this paper, we make use of the fact that most of the In phases of the Cu-In-S system have noncubic lattice structures at room temperature (RT). Hence, there will exist one well-defined EFG for each crystallographically equivalent In site in such a phase. By means of a single-phase specimen it is therefore possible to characterize the In sites and to determine their relative population at a precision of typically $\pm 1\%$. Once the PAC signatures of all In phases of a system (at a given temperature) are known, mixed-phase samples can be analyzed for the contributing In phases and their relative fractions. However, in the present type of experiment, PAC's are not sensitive to Cu and to the Cu-S phases.

After a description of the sample preparation employed and a brief outline of the PAC technique and data analysis in Sec. II we shall discuss the results obtained for the single- and mixed-phase samples in Sec. III.

II. EXPERIMENTAL DETAILS

A. Sample preparations

The PAC tracer ^{111}In-^{111}Cd was chosen for the present investigation since the radioactive ^{111}In atoms are chemically indistinguishable from the overwhelming majority of the inactive indium atoms. Using metallic indium, containing statistically distributed ^{111}In, as one of the starting materials for crystal growth, the ^{111}In atoms occupied the available In sites with the same probability as the inactive In atoms in all grown crystals. Hence, PAC's generate a precise representative survey of the local indium environments. We point out that this is generally not true if common doping techniques are applied which make use of implantation or diffusion of ^{111}In into already existing samples.

The copper, indium, and sulfur starting materials were of 6N purity (Ventron Corp.). The sulfur was outgassed at 10^{-6} mbar immediately before use. Appropriate amounts of these materials were weighed out in order to obtain the desired composition. A typical sample weight was 5 g. ^{111}In was obtained in amounts of 2 mCi as $^{111}InCl_3$ in 0.04 molar HCl in aqueous solution from Amersham-Buchler Corp. For one preparation procedure about $\frac{1}{10}$th of the activity was dripped onto a high-purity indium foil and the water was removed by moderate heating. The foil was melted under a H_2 atmosphere in order to reduce the ^{111}In and achieve a statistical distribution of ^{111}In in indium. Subsequently the solidified indium droplet was etched in concentrated HCl. A PAC measurement showed the signal of metallic In for 99(1)% of the probes and thus proved the full success of the incorporation procedure used. The radioactively prepared indium metal together with one or two of the other elements was properly positioned in a quartz ampoule which was then sealed under argon atmosphere. Thus most samples were directly produced from the constituent elements and all samples were grown from the melt. All sulfur compounds were produced in a two-zone furnace in which the sulfur was positioned at the low-temperature end ($T \simeq 500$ °C). A typical setup is shown in Fig. 1(a). Figure 1(b) shows the temperature profile within the oven which developed upon heating one zone only. Some samples were rapidly quenched from the melt to RT. Annealing treatments were employed in order to test whether the results corresponded to equilibrium conditions. More details of the preparation techniques are discussed below in Sec. III.

B. PAC and data analysis

Perturbed angular correlations of γ rays were observed for the 171–245-keV γ cascade of ^{111}Cd which follows the electron-capture decay of ^{111}In (half-life 2.8 d). Thus the nuclear quadrupole interaction of the isomeric $\frac{5}{2}^+$ state (half-life 85 ns) of ^{111}Cd with surrounding charges was observed. The measured quantity is the traceless electric-field-gradient tensor $eq_{x^{(i)}x^{(j)}}$ where e is the elementary charge and $x^{(i)}$ and $x^{(j)}$ are Cartesian coordinates. The largest component, eq_{zz} (the "strength" of the EFG), and the dimensionless asymmetry parameter, $\eta \equiv (q_{xx}-q_{yy})/q_{zz}$ (the "symmetry" of the EFG), completely describe the EFG tensor in its diagonalized form. The orientation of the principal axes of the EFG tensor, within the coordinate system of a single crystalline sample, can be expressed by means of the three Euler angles. In the present investigation, only polycrystalline specimens were used, and therefore the orientation of the EFG tensor could not be determined. We use the quadrupole interaction frequency $\nu_Q \equiv e^2 q_{zz} Q/h$ [eQ is the electric quadrupole moment of the probe with $Q = 0.83 \times 10^{-28}$ m^2 (Ref. 10) and h denotes the Planck constant] and the asymmetry parameter η (by definition: $0 \le \eta \le 1$) to characterize one In site. A site of cubic symmetry yields $\nu_Q = 0$, while a site of at least threefold axial symmetry leads to $\eta = 0$. Using a conventional four-detector setup[11] we measured 12 delayed coincidence spectra $C_{ij}(\Theta, t)$ where i,j denotes the counter number ($i \neq j$), $\Theta = 90°$ or 180° stands for the angle between the counters of a coincidence pair, and t is the delay time between the emission of the two γ quanta. The exponential decay function and counter asymmetries are eliminated by forming the experimental counting rate ratio, $R_{\text{expt}}(t)$, which reads:[11]

$$R_{\text{expt}}(t) = \frac{2}{3}\left[\frac{(C_{13}C_{31}C_{24}C_{42})^{1/4}}{(C_{12}C_{21}C_{23}C_{32}C_{34}C_{43}C_{41}C_{14})^{1/8}} - 1\right] . \quad (1)$$

Since the probes may, in general, occupy N different sites numbered by $i = 0, 1, \ldots, N$ the theoretically expected

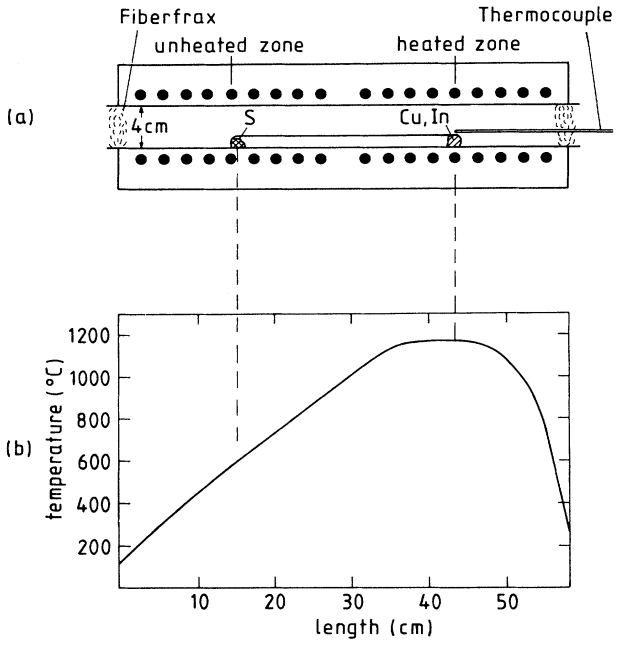

FIG. 1. (a) Two-zone furnace for the preparation of Cu-In-S samples. The elements are sealed for a quartz ampoule under Ar atmosphere. (b) Temperature profile inside the furnace which develops when one zone only is heated to 1100 °C.

PAC spectrum, $R_{\text{theor}}(t)$, takes the following form:[9]

$$R_{\text{theor}}(t)=A_{22}\sum_{i=0}^{N} f_i \sum_{n=0}^{3} s_{ni}\exp(-c_{ni}b_i t) \times\cos[(3\pi/10)c_{ni}\nu_{Qi}t]\ . \quad (2)$$

$A_{22}=-0.179$ is the anisotropy coefficient of the employed γ cascade. The experimentally observed anisotropies are somewhat reduced due mainly to the finite solid angles of the γ counters. Each defect site or local environment, i, is occupied with the probability f_i and contributes to the spectrum with three frequencies, $c_{ni}\nu_{Qi}$, which are weighted by the amplitudes s_{ni}. The parameters c_{ni} and s_{ni} depend on η_i. Throughout the text, the non cubic sites of a single compound are numbered by $i=1,2,3,\ldots$, while $i=0$ always refers to sites of cubic symmetry. Sometimes an otherwise well-defined probe environment is slightly perturbed by distance and statistically distributed lattice defects. It was empirically found that this situation can be accounted for by assuming a Lorentzian frequency distribution around ν_{Qi} with a full width at half maximum (FWHM) of $2b_i$.[12] The latter gives rise to the exponential term in Eq. (2). Commonly, a PAC spectrum obtained via Eq. (1) is least-squares fitted to determine the parameters of Eq. (2). Sometimes it is also convenient to visualize the contributing frequencies by means of a Fourier transform.[13]

C. Supplementary experiments

In most cases PAC measurements yield a precise signature of a phase without, however, providing direct experimental access to the lattice structure. Therefore, we additionally performed x-ray-diffraction (XRD) measurements on samples which had been used in the PAC experiments. Since these measurements could be done only after a practically complete decay of the ^{111}In radioactivity, i.e., more than one month after preparation, we also produced samples without ^{111}In but under otherwise identical conditions compared to those employed for the PAC samples. Thus, we are able to compare the PAC data to the large body of XRD data from the literature and check the consistency of the results. In some cases, samples were also characterized by energy dispersive x-ray fluorescence (EDX) or by their electrical properties.

III. RESULTS AND DISCUSSION

A. Copper-indium phases

According to a compilation by Massalski[14] there exist three intermetallic copper-indium phases at RT named δ, η, and ϕ phases. The ϕ phase, however, is not mentioned in the most recent assessment.[15] The hitherto unknown $CuIn_2$ phase was discovered by Keppner *et al.* in an ingenious PAC experiment at the interface between thin evaporated copper and indium films[16] The PAC signal of ^{111}In in In is well-known[10,11] (see Table I).

We carried out experiments to identify the δ, η, and ϕ phases by their hyperfine parameters, to find out whether the $CuIn_2$ phase would also appear in bulk material, and to search for additional unknown copper-indium phases.

Samples having the compositions $Cu_{70.5}In_{29.5}$ (δ phase), $Cu_{64}In_{36}$ (η phase), $Cu_{58.5}In_{41.5}$ (ϕ phase), and $Cu_{33.3}In_{66.7}$ ($CuIn_2$ phase) were produced from weighed amounts of Cu and In containing ^{111}In. Sealed under Ar atmosphere in a quartz ampoule the compounds were melted for 3 h at 900 °C or 800 ° C ($Cu_{64}In_{36}$) and then quenched to room temperature. PAC spectra were recorded before and after a subsequent annealing procedure. Samples with compositions $Cu_{45}In_{55}$ (composition *F*), $Cu_{25}In_{75}$ (composition *G*), and $Cu_{10}In_{90}$ (composition *H*) were produced by successively adding inactive In to the $Cu_{58.5}In_{41.5}$ compound, melting, and quenching to RT. These samples were not annealed.

Shown in Fig. 2(a) is the PAC spectrum obtained for the δ phase ($Cu_{70.5}In_{29.5}$) after annealing at 500 °C. The solid line represents a least-squares fit to the data using Eq. (2). We find one cubic ($\nu_Q=0$) and three noncubic sites. The respective parameters are given in Table I. Within the limits of error, the same parameters were obtained from the PAC spectrum measured before annealing, indicating that the data refer to an equilibrium state.

According to the most recent assessment[15] the δ phase (Cu_7In_3) is a homogeneous phase for In atomic fractions between 29.0% and 30.6%. It has a complex structure which led to different assignments of the type of lattice.[17–19] More recent investigations assume a triclinic structure having 40 atoms in the unit cell.[20,21] Our PAC data show four well-resolved In sites, one of which has cubic symmetry. This clear-cut signature will allow recognition of the phase by means of its PAC parameters. The XRD spectrum revealed good agreement with a theoretical pattern calculated using the structure data of Ref. 20 indicating that indeed the δ phase was present.

The PAC spectrum of the η phase ($Cu_{64}In_{36}$) is shown in Fig. 2(b) while the respective parameters are included in Table I. After annealing at 500 °C, the sample was ground in a mortar in order to avoid texture effects. We find two noncubic In sites with approximately equal population. A characteristic feature of both sites is the relatively broad distribution of the quadrupole interaction frequencies.

The η phase (Cu_2In) has a filled NiAs-type structure.[22] According to Jain, Ellner, and Schubert[23] the η phase splits into at least five phases having different superstructures due to different ordering of the vacancies. The detailed copper-indium phase diagram between 32.9 and 37.8 at. % In can be found in Ref. 23. XRD spectra proved that we had produced a sample with NiAs-type structure with a superstructure that did not correspond to the phases *A* and *A'* of Ref. 23 but which possibly coincides with the *B* phase of that reference.

Figure 2(c) shows the PAC spectrum for the composition $Cu_{58.5}In_{41.5}$ (ϕ phase) after annealing at 280 °C. The PAC parameters of the two resolved In sites are included in Table I. Before annealing, the spectrum contained two additional components: one with $\nu_Q=17(1)$ MHz and $\eta=0$, which is due to ^{111}In in In, and another one with $\nu_Q=149(2)$ MHz and $\eta=0.21(2)$ which could not be identified. The facts that these components vanish upon

annealing and that the parameters of the remaining components are distinctly different from those obtained for the η phase indicate the formation of a homogeneous phase which is different from the η phase. XRD shows that the structure of this phase is also of the NiAs type.

In older works, a homogeneity range between 41 and 41.5 at. % In is assumed for the so-called ϕ phase. Rajasekharan and Schubert[24] propose a phase of NiAs-type structure with a homogeneity range between 43.5 and 44.5 at. % In ($Cu_{11}In_9$). It is assumed that this phase is stable only above 156 °C.[15] According to these authors, the ϕ phase does not exist. Hence, having a sample of $Cu_{58.5}In_{41.5}$ we should have observed a mixture of In and the η phase. This was, however, not the case. We hoped to resolve this discrepancy by means of a sample of the composition $Cu_{56}In_{44}$ which, however, also only yielded the PAC parameters of the ϕ phase (see Table I). Hence, the PAC data suggest that the ϕ phase, which is not identical to the η phase or one of its modifications, does exist, at least as a metastable phase, at RT and has a broad homogeneity range. The designation as ϕ phase is retained throughout the text.

Shown in Fig. 3(a) is the Fourier transform of a PAC spectrum measured for a sample of the composition $Cu_{33.3}In_{66.7}$ after quenching from the melt. Three triplets of quadrupole frequencies appear in that transform. No. 1 corresponds to metallic indium while the components Nos. 2 and 3 are identical to those of the ϕ phase. This result is expected if no other Cu-In phases existed between $\simeq$45 and 100 at. % In. However, after annealing the sample at 87 °C for 4.5 d, the additional frequency set No. 4 appears [see Fig. 3(b)]. The corresponding parameters agree with those given by Keppner *et al.* for the $CuIn_2$ compound.[16] We assume that a prolonged annealing procedure would have led to the complete conversion into this phase. Unfortunately, the half-life of ^{111}In im-

TABLE I. PAC signatures of the In phases of the Cu-In-S system at RT. The parameters refer to Eq. (2). Values without error were kept fixed during least-squares fit.

Phase	Site No. (index i)	ν_{Qi} (MHz)	η_i	b_i (MHz)	f_i (%)	Ref.
$CuInS_2$	0	0		0.2(1)	100	Ref. 6
$CuIn_5S_8$	1	7(1)	0.00(1)	0.7	85(5)	This work
	2	47(10)	0.00(5)	20(1)	15(5)	
Cu-In	0	0		0.1(1)	24(6)	This work
(δ phase)	1	80(1)	1.00(1)	0.0	13(1)	
	2	126(1)	0.56(1)	4.0	20(2)	
	3	144(1)	0.30(1)	2(2)	43(3)	
Cu-In	1	158(1)	0.37(1)	18.4	52(2)	This work
(η phase)	2	171(1)	1.00(2)	19(7)	48(2)	
Cu-In	1	130(1)	0.92(2)	98(4)	84(4)	This work
(ϕ phase)	2	165(1)	0.22(2)	11(9)	16(3)	
$CuIn_2$[a]	1	85(1)	0.57(1)	0	100	Ref. 16, This work
In	1	18(1)	0.01	0	100	Ref. 11
InS	1	233(1)	0.14	1	100	Ref. 27
In_6S_7	1[b]				$\simeq$60	This work
	2[c]				$\simeq$40	
$In_{2.8}S_4$[d]	0	0			100	Ref. 27
β-In_2S_3	1	142(1)	0.01	2	23(3)	Ref. 27
	2	60(1)	0.06	2	77(3)	

[a]Not produced as a single phase in the present work.
[b]Sites with fast relaxation, which leads to loss of γ anisotropy.
[c]Sites characterized by 11 lines in Fourier spectrum (Fig. 4).
[d]Phase identical to α-In_2S_3.

poses a practical limit of several days for annealing times in these PAC experiments.

The compound $CuIn_2$ is to date not mentioned in any of the investigations or compilations of the Cu-In phase diagram which were available to the authors. Keppner *et al.* performed PAC experiments using a thin film of indium doped with ^{111}In which was evaporated onto a thin copper film.[16] At low temperatures they observed the signal of metallic indium (see Table I). This signal gradually vanished at the expense of a hitherto unknown PAC signal during the course of an isochronal thermal annealing sequence between $-70\,°C$ and $87\,°C$. The new signal was attributed to the formation of an intermetallic phase which occurred through a thermally activated solid-state reaction. A quantitative comparison of phase fractions obtained from PAC and film thickness allowed the determination of the 1:2 stoichiometry of the phase. Our results now show that $CuIn_2$ also appears as a stable phase in bulk material. The well-defined PAC signal of $CuIn_2$ [there is no spread in the quadrupole frequency, i.e., $b_1=0$, refer to Eq. (2)] shows that this phase occurs in large grains with an undetectably low number of structural defects. In comparison to the thin-film experiment, the formation of this phase occurs from the decomposition of the neighboring ϕ phase and In. This means that the formation of the $CuIn_2$ phase in contact with Cu and In in the thin-film experiment does not correspond to bulk equilibrium conditions. $CuIn_2$ exhibits a tetragonal structure of $CuAl_2$ type with lattice parameters $a=6.65$ Å and $c=5.38$ Å.[16] Our XRD measurements confirm these results. Moreover, a comparison of our XRD data for $CuIn_2$ to the XRD data published by Simic and Marinkovic[25] reveals that the Cu-In phase of these authors, with the assumed atomic Cu to In ratio of 1:1, is identical to the $CuIn_2$ phase.

The samples of the compositions $Cu_{45}In_{55}$, $Cu_{25}In_{75}$, and $Cu_{10}In_{90}$ all yield the signals of the ϕ phase and of metallic In (see Table I). Hence, there is no indication for additional Cu-In phases. In accordance with the observation discussed above, the $CuIn_2$ phase did not appear in these experiments due to the high cooling rates during sample production.

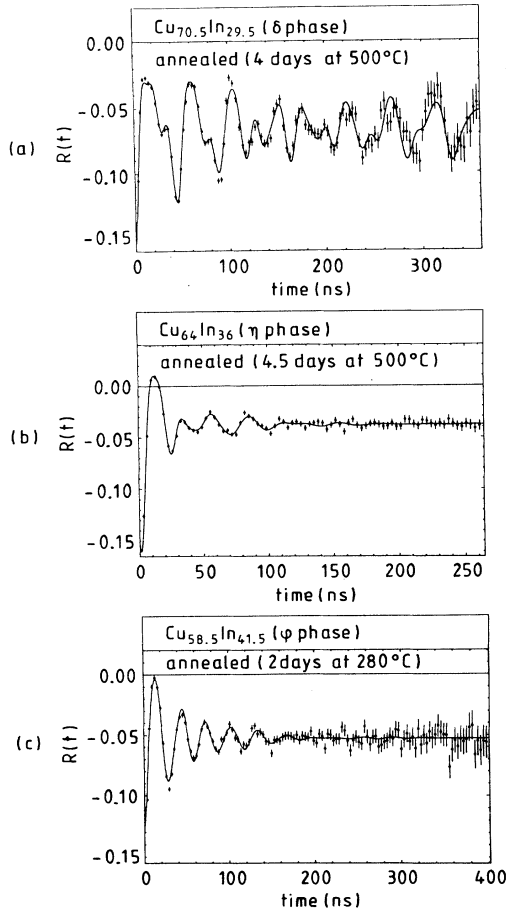

FIG. 2. PAC spectra obtained for Cu-In δ phase (a), η phase (b), and ϕ phase (c). The pronounced modulations in all spectra are due to at least two noncubic In sites in all three phases. The solid lines represent least-squares fits to the data according to Eq.. (2), the parameters of which are listed in Table I.

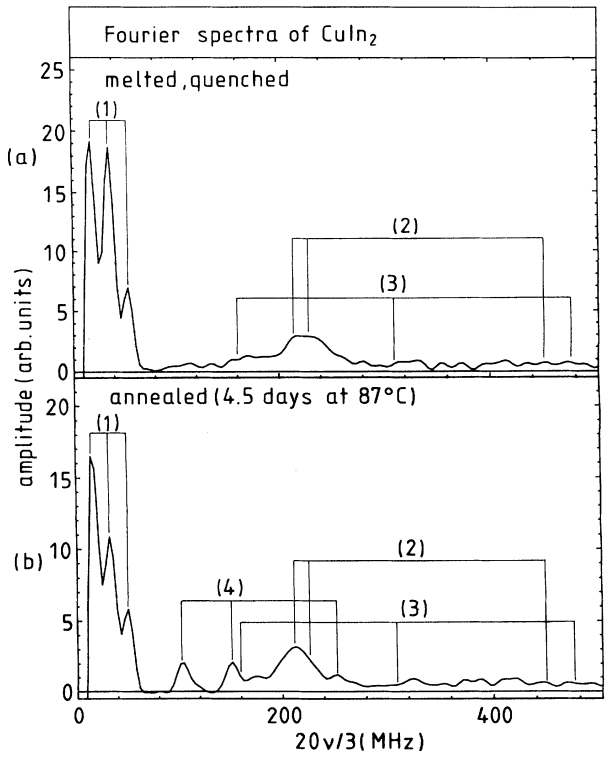

FIG. 3. Fourier transforms of PAC spectra measured for $Cu_{33.3}In_{66.7}$ as prepared (a) and after annealing (b) at 87 °C for several days. Spectrum (a) reveals the appearance of three sets of quadrupole frequencies, Nos. 1, 2, and 3, which correspond to metallic In (No. 1) and to the Cu-In ϕ phase (Nos. 2 and 3). As shown in (b) an additional frequency set No. 4 appears after annealing. The respective parameters agree with those previously determined for the $CuIn_2$ phase (see Table I).

B. Indium-sulfur phases

The stable phases of the In-S system at RT are InS, In_6S_7, $In_{2.8}S_4$, and In_2S_3.[26] The PAC parameters of InS and β-In_2S_3, the RT modification of In_2S_3, have already been determined by Frank *et al.*[27] The phase $In_{2.8}S_4$ is identical to the high-temperature modification of In_2S_3 (α-In_2S_3, $414\,^{\circ}C < T < 750\,^{\circ}C$), which, in the given stoichiometry, is stable down to RT and has cubic symmetry (see Table I). Therefore we only studied the In_6S_7 compound in this work. Figure 4(a) shows the PAC time spectrum recorded for this sample after quenching to RT as well as the spectrum observed after a subsequent annealing treatment. Figure 4(b) displays the respective Fourier transforms. The time spectra show that, in both cases, about 60% of the probe nuclei undergo a fast relaxation process which reduces the observable γ anisotropy to about -0.08. The quadrupole interaction of the remaining probes gives rise to a very complex modulation which leads to the appearance of 11 significant lines in the Fourier spectrum, indicated by arrows in Fig. 4(b). As a consequence, it was not possible to obtain a satisfactory fit to the data and so we cannot determine the underlying PAC parameters. Instead, we chose to use the characteristic Fourier spectrum for the recognition of the In_6S_7 phase.

The compound In_6S_7 belongs to the III-VI family of semiconductors and has a monoclinic lattice structure with 26 atoms per unit cell.[28,29] The fast relaxation process observed by PAC's (60% of the probe nuclei) is a phenomenon typical for decay after effects in insulators.[11] Therefore, we assume that the material grown here is semi-insulating. The PAC modulation of the remaining probes reflects the complex lattice structure of the compound which has, according to the number of lines in the Fourier spectrum, at least four different In sites.

C. Copper-indium-sulfur phases

$CuInS_2$ and $CuIn_5S_8$ are the only known ternary phases of the Cu-In-S system. They both belong to the Cu_2S-In_2S_3 quasibinary section which was thoroughly investigated by Binsma, Giling, and Bloem.[30] Stoichiometric samples of both $CuInS_2$ and $CuIn_5S_8$ were produced and characterized by PAC's.

For $CuInS_2$ we find perfect cubic symmetry of the local environment around the normal In site, which is occupied by more than 99.5% of the probes.[6] Hence, the EFG which was deduced for this site by NMR measurements[31] using the isotope ^{115}In could not be confirmed. More details concerning the EFG in $CuInS_2$ can be found in Ref. 32. For the present discussion it is sufficient to note that the $CuInS_2$ compound always yielded $\nu_Q = 0$ and a narrow distribution of low quadrupole frequencies as described by the parameter b_0 [refer to Eq. (2) and Table I]. XRD measurements confirmed that single-phase $CuInS_2$ had been prepared. An electrochemical measurement yielded n-type conductivity, as expected for the stoichiometric compound.[33]

The PAC spectrum of $CuIn_5S_8$ is shown in Fig. 5. The spectrum was fitted (solid line) by assuming two axially symmetric EFG's ($\eta = 0$). The parameters are listed in Table I. The site with the higher EFG is also characterized by a very broad distribution of quadrupole frequen-

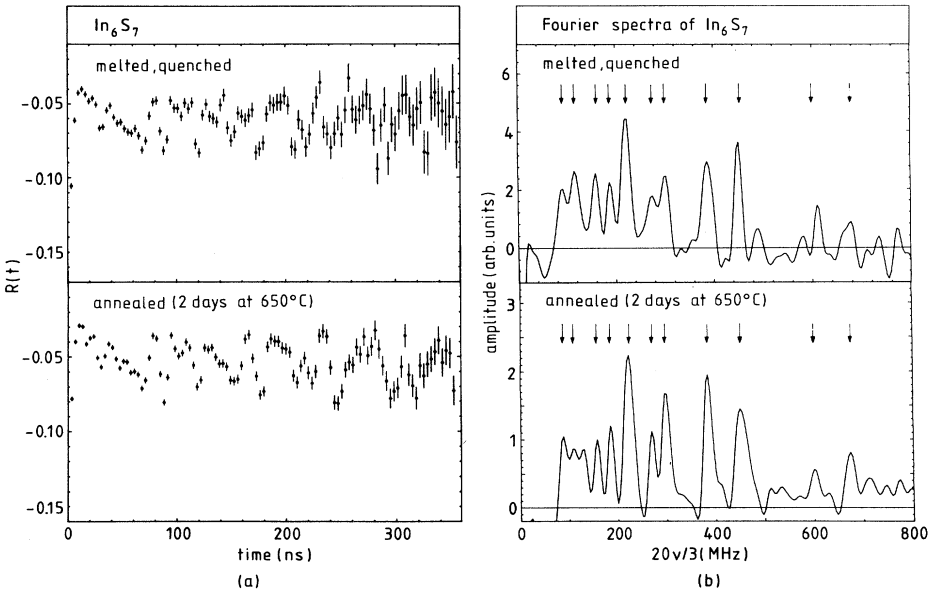

FIG. 4. PAC spectra (a) and their Fourier transforms (b) of In_6S_7 as prepared (top) and after annealing at 650 °C (bottom). As visible in the time spectra (a), in both cases a fast relaxation process occurs for $\simeq 60\%$ of the probes, which reduces the observable γ anisotropy to -0.08. The remaining probes ($\simeq 40\%$) show a complicated modulation which gives rise to eleven significant peaks (marked by arrows) in the Fourier spectra (b). This characteristic pattern is directly taken as the signature of the In_6S_7 compound.

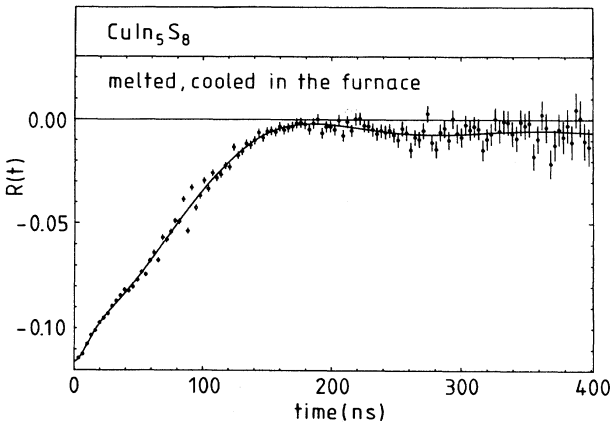

FIG. 5. PAC spectrum of stoichiometric $CuIn_5S_8$. The two noncubic In sites of the normal spinel structure of this compound (Ref. 34) give rise to two probe fractions with axially symmetric EFG's. The expected occupation numbers for these sites (Ref. 34) match well with the respective fractions observed in the PAC spectrum.

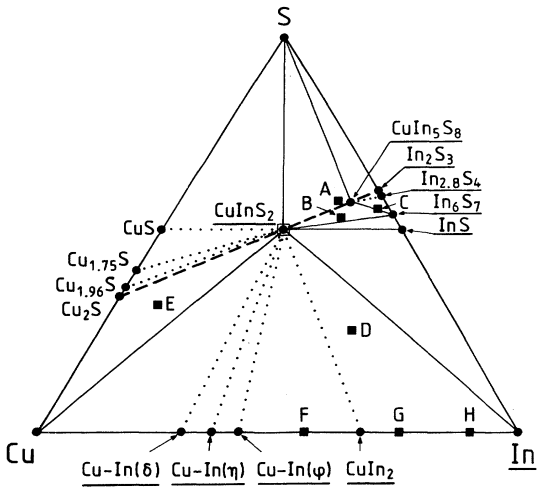

FIG. 6. Gibbs phase triangle of the Cu-In-S system at RT. Full circles denote the phases of the system. The PAC signatures of the underlined phases are known from the literature or were determined in the present work (see Table I). The dashed line between Cu_2S and In_2S_3 corresponds to a quasibinary section which was investigated by Binsma, Giling, and Bloem (Ref. 30). The full squares $A-H$ describe compositions of mixed-phase samples which were employed in order to determine new tie lines (full lines within the Cu-In-S triangle). Other tie lines (dotted lines) are suggested by the present work.

cies with a FWHM $\equiv 2b_2 \simeq \nu_{Q2}$.

$CuIn_5S_8$ crystallizes in the normal spinel structure with $a = 10.698$ Å.[34] Compounds of this structure usually have the stoichiometry AB_2C_4 where A and B denote metallic ions which, respectively, occupy $\frac{1}{8}$ and $\frac{1}{2}$ of the tetrahedrally (A-site) and octahedrally (B-site) coordinated gaps in the close-packed structure of the C ions. According to Flahaut *et al.*, the A sites in $CuIn_5S_8$ are occupied equally by Cu and In atoms, while all B sites are occupied by In atoms. Hence, in the present case, the formula AB_2C_4 becomes $(Cu_{0.5}In_{0.5})\,In_2S_4$, which is equal to $\frac{1}{2}CuIn_5S_8$. This means that 20% of the ^{111}In probes should be located on A sites while 80% are expected to be on B sites. Within the limits of error the fractions f_2 and f_1 (see Table I) are compatible with these expectations. Therefore, we assign $\nu_{Q2} = 47$ MHz to the tetrahedral A site and $\nu_{Q1} = 7$ MHz to the octahedral B site. Indeed, a smaller EFG is expected for the larger octahedrally coordinated gap. The broad distribution of quadrupole frequencies, observed for the tetrahedral site, indicates large statistically distributed deviations from the ideal symmetry. The XRD spectrum of our sample showed a good agreement with literature data.[34,35] A electrochemical measurement demonstrated n-type conductivity for this sample.

D. Phase relations

Figure 6 shows the Gibbs phase triangle of the Cu-In-S system at RT. It contains all known phases of this system. The PAC signatures of the underlined phases were either determined in the present work or are known from the literature (see Table I). Hence, the recognition of these phases, i.e., of all phases that contain In, is possible through PAC measurements. The phase triangle is divided into subtriangles by tie lines which reflect phase equilibria. The tie line between Cu_2S and In_2S_3 (broken line) follows from the investigations of Binsma, Giling, and Bloem.[30] New tie lines were determined (solid lines) or suggested (dotted lines) by the results of the present PAC investigations using mixed-phase samples of chosen compositions which correspond to the points $A-H$. In the following, we outline the results obtained with the compositions $A-E$. The results obtained for the compositions F, G, and H have already been discussed in Sec. III A.

Composition A corresponds to $Cu_9In_{33.5}S_{57.5}$. The sample was produced in a closed ampoule from $CuInS_2$, In containing ^{111}In, and S in a two-zone furnace with the sulfur at 600 °C and the other materials at 1170 °C (12 h) and 1200 °C (2 h). Despite the long reaction time the sulfur did not completely react with the melt and considerable amounts of elemental sulfur were visible to the naked eye after the ampoule had cooled down to RT. The PAC spectrum yields a cubic fraction ($\nu_Q = 0$) for 22(2)% of the probes which we attributed to $CuInS_2$. The remaining fraction could be fitted with the parameters of $CuIn_5S_8$ (see Table I) using a ratio of 2:1 in the relative populations of the two In sites of this compound, rather than the expected 4:1 ratio for the stoichiometric case (see also Sec. III C and Ref. 34). This shows that large variations in the relative occupations of the two In sites in $CuIn_5S_8$ are possible. The presence of $CuInS_2$ and $CuIn_5S_8$ was confirmed by XRD. The coexistence of $CuInS_2$, $CuIn_5S_8$, and S in thermal equilibrium proves the existence of the tie lines S-$CuInS_2$ and S-$CuIn_5S_8$ (see Fig. 6).

Figure 7 shows the PAC spectrum measured for a sample of the composition $Cu_{11}In_{35}S_{54}$ (composition *B*) which had been produced from the elements, quenched to RT, and annealed at 650 °C (3 d). The quenched sample (top of Fig. 7) reveals a cubic fraction with $f_0=21(3)\%$ that stems from $CuInS_2$, while 11(1)% of the probes show the modulation of InS, and the remaining signal is due to $CuIn_5S_8$. The relative occupation of the In sites in the latter compound is now 4:3 instead of 4:1. After annealing at 650 °C (bottom of Fig. 7) the modulation of InS has vanished and only the increased cubic fraction of $CuInS_2$ [$f_0=34(3)\%$] and the fraction of $CuIn_5S_8$ (with a 1:1 occupation of the In sites) are present. The observed behavior indicates that the results of the quenched sample do not correspond to equilibrium. A feature of both spectra is the relatively low observed γ anisotropy of -0.13. Taking into account a distance of 10 cm between γ detectors and sample the expected value of -0.16. XRD showed that the annealed sample contained the compound In_6S_7 in addition to $CuInS_2$ and $CuIn_5S_8$, although the complex modulation of In_6S_7 (see Fig. 4) is clearly absent from the PAC spectrum. We assume that the fast relaxation process, which occurred for 60% of the probes in single-phase In_6S_7, now affects all probes due to an uncontrolled change in the electronic properties of the compound. This view is confirmed by the observed low γ anisotropies which, in this case, are the only PAC based indications for the presence of In_6S_7. The simultaneous appearance of $CuInS_2$, In_6S_7, and $CuIn_5S_8$ determines the tie lines $CuInS_2$-In_6S_7 and In_6S_7-$CuIn_5S_8$.

The production of $Cu_{2.5}In_{42}S_{55.5}$ (composition *C*) was performed via the melting of weighed amounts of $CuInS_2$, In_2S_3, and ^{111}In-containing In. PAC's were measured after cooling to RT as well as after annealing at 650 °C. The PAC time spectrum obtained after annealing could not be fitted in a satisfactory way. Therefore, we show in Fig. 8 only the Fourier spectra. Considerable differences are visible. Before annealing the spectrum is dominated by the component No. 1, which is characterized by a broad distribution of $b_1\simeq 35$ MHz around a quadrupole frequency of $\nu_{Q1}=60(2)$ MHz ($\eta_1=0$) with $f_1=73(2)\%$. Besides this, a cubic component [$f_0=10(2)\%$] and a well-defined quadrupole component No. 2 with $\nu_{Q2}=233(4)$ MHz [$\eta_2=0.15(1)$] and $f_2=17(1)\%$ appear. (Note, that a cubic component does not appear in the Fourier spectrum.) The cubic part is probably due to

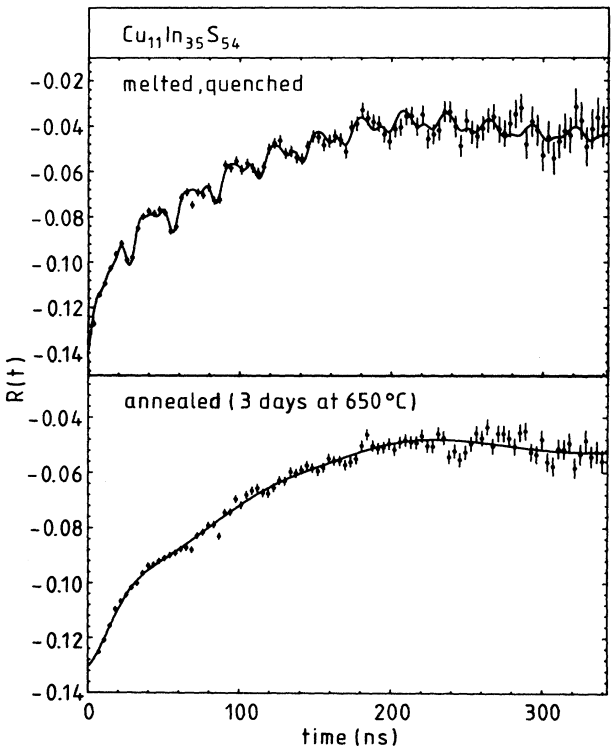

FIG. 7. PAC spectrum of the sample of composition *B* as prepared (top) and after annealing (bottom). The fast modulation in the upper spectrum is due to InS and vanishes during annealing. A cubic part due to $CuInS_2$ and the signature of $CuIn_5S_8$ remain after annealing (bottom). However, the appearance of In_6S_7 in this case can only indirectly be inferred from a somewhat reduced γ anisotropy compared to the expected value of -0.16.

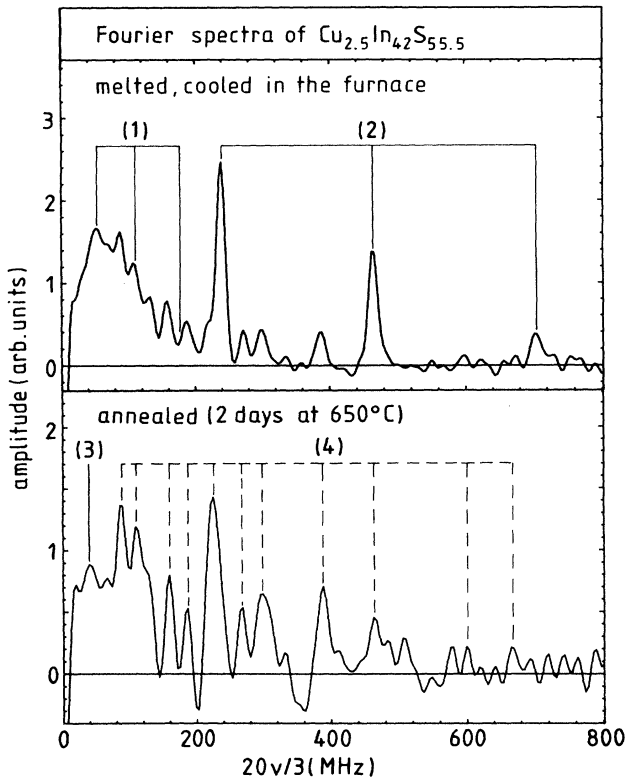

FIG. 8. Fourier transform of the PAC spectrum obtained for composition *C* as prepared (top) and after annealing (bottom). Before annealing (top) the dominating In site in β-In_2S_3 (component No. 1), InS (component No. 2), and a cubic part (not visible in the Fourier spectrum) due to $In_{2.8}S_4$ (β-In_2S_3) are present. After annealing In_6S_7 (component No. 4) and component No. 3 become visible. The latter corresponds to an In site in $CuIn_5S_8$.

$In_{2.8}S_4$ being identical to α-In_2S_3, while component No. 1 corresponds to the dominating In site in β-In_2S_3 and component No. 2 to InS. The result after annealing indicates that this mixture of phases does not represent equilibrium. The Fourier spectrum [Fig. 8 (bottom)] now shows two completely different components, Nos. 3 and 4. Component No. 4 is identical to the pattern of 11 lines, which is the signature of the In_6S_7 compound (see Fig. 4 and Sec. III B). Component No. 3 belongs to a quadrupole frequency with $\nu_Q \simeq 42$ MHz, which is compatible with the *A* site in $CuIn_5S_8$ (see Sec. III C). In fact, XRD indicates the appearance of In_6S_7 and $CuIn_5S_8$. However, the quadrupole frequencies of the dominating *B* site of $CuIn_5S_8$ [$\nu_{Q1}=7(1)$ MHz] do not appear in the PAC Fourier spectrum. Instead, a considerable cubic component ($f_0 \simeq 15\%$) is still present in the time spectrum. The corresponding probe fraction cannot be assigned to $In_{2.8}S_4$ or $CuInS_2$, which are the only cubic In phases of the system at RT, since composition *C* lies only slightly above the tie line between $CuIn_5S_8$ and In_6S_7. One solution to this problem is to assume that the *B* site of $CuIn_5S_8$ can also occur with vanishing EFG. The simultaneous appearance of $CuIn_5S_8$ and In_6S_7 confirms the tie line between these compounds. This line suggests that the tie line between $In_{2.8}S_4$ and $CuIn_5S_8$ exists also.

$Cu_{23}In_{52}S_{25}$ (composition *D*) was produced by melting weighed amounts of Cu, In_2S_3, and In containing ^{111}In at 1150 °C. Subsequently the sample was cooled to RT and annealed at 130 °C. Shown in Fig. 9 are the respective PAC time spectra which were fitted using a cubic component that we assign to $CuInS_2$ [$f_0=16(1)\%$], the parameters of In [$f_1=79(1)\%$], and the remaining fraction using the modulation due to the Cu-In ϕ phase. The given fractions refer to the sample after annealing. We assume that the $CuIn_2$ compound did not appear in this experiment since the annealing temperature of 130 °C lies above the temperature of decomposition for this compound. During cooling of RT it was probably not formed in significant amounts due to the long time needed for its formation (see also Sec. III A). The results of composition *D* suggest a tie line between the Cu-In ϕ phase and $CuInS_2$ and confirm the tie line In-$CuInS_2$.[6]

A sample with the composition $Cu_{60}In_9S_{31}$ (composition *E*) was prepared in the same way as $CuInS_2$, cooled at RT, and annealed at 620 °C. The PAC spectra before and after the annealing treatment are dominated by a heavily perturbed cubic component which is assigned to $CuInS_2$. A minor fraction of 17% with $\nu_Q=143(2)$ MHz [$\eta=0.29(1)$] nearly vanishes upon annealing. This fraction corresponds to the dominant In site in the Cu-In δ phase. Its strong decrease upon annealing indicates that the δ phase is not an equilibrium phase at this composition. An EDX analysis of the sample showed the presence of small Cu precipitates. The coexistence of $CuInS_2$ and Cu as equilibrium phases proves the existence of the tie line Cu-$CuInS_2$. This line is in contradiction to the tie line between Cu_2S and a Cu-In phase assumed by Binsma,[36] rather it confirms earlier observations of the same author.[30] The tie line Cu-$CuInS_2$ is also in agreement with recent investigations performed in our group.[37]

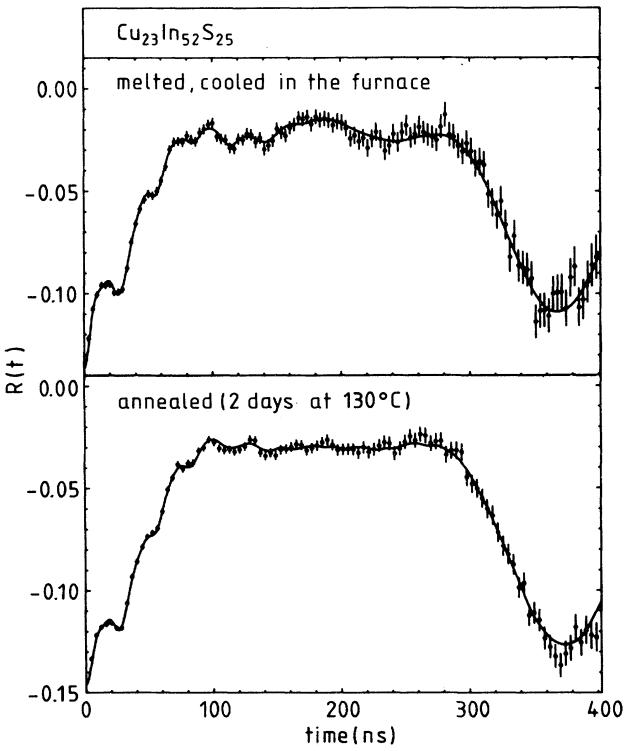

FIG. 9. PAC spectra of the sample having composition *D*. The spectra of the as-prepared state (top) and of the sample after annealing (bottom) are identical within the limits of error. Both spectra reveal a cubic part due to $CuInS_2$, a slow modulation induced by metallic In, and a fast modulation with the parameters of the Cu-In ϕ phase.

IV. CONCLUSIONS

It was demonstrated that PAC's are well suited to characterize phases and to determine phase relations in the Cu-In-S system.

We identified in the Cu-In subsystem by means of their PAC parameters the δ, η, and ϕ phases. The ϕ phase was shown to be identical with the phase $Cu_{11}In_9$ of Ref. 24 and is probably metastable at RT. The phase $CuIn_2$ was hitherto known only from a PAC experiment on thin-film interfaces.[16] Our results establish this phase as a stable bulk phase whose formation from the neighboring ϕ phase and In was observed. The decomposition temperature of $CuIn_2$ in bulk material is below 130 °C, which makes it easy to understand why this phase was not discovered earlier, although analogous phases exist in similar systems, e.g., $AgIn_2$.[38] We found no indication for the existence of additional phases in the Cu-In system at RT. In particular, there is no Cu-In phase with a 1:1 atomic ratio. Hence, the production of stoichiometric $CuInS_2$ via the sulfurization of a metallic sample cannot start from a single metallic phase.

The PAC signature of the phase In_6S_7 is a pattern of 11 lines in the Fourier transform of the PAC time spectrum. The complexity of the spectrum did not allow the reliable evaluation of the underlying hyperfine parameters.

$CuInS_2$ and $CuIn_5S_8$ are the only ternary phases of the Cu-In-S system that are stable at RT. The normal In site in $CuInS_2$ has perfect cubic symmetry and no indication of a tetragonal distortion of the chalcopyrite structure of this compound is found by PAC's.[6] The presence of two noncubic In sites in $CuIn_5S_8$ with approximately the same populations as suggested earlier[23] is confirmed by PAC's. However, the relative occupation of these two sites may vary widely when the compound is produced in equilibrium with other phases.

Combined with the previously determined PAC parameters of $CuIn_2$, In, InS, $In_{2.8}S_4$ (α-In_2S_3), and β-In_2S_3 our data constitute the first complete set of PAC signatures for the indium containing phases of a ternary system. The data (and references) are collected in Table I.

Our data, determined from measurements of mixed-phase samples of chosen compositions, show the existence of seven tie lines in the Gibbs phase triangle (solid lines in Fig. 6). The existence of several other tie lines (dotted lines in Fig. 6) can also be postulated with high probability. Calculations performed by Migge show that the phase relations determined and suggested in the present work are fully self-consistent and are in agreement with existing thermodynamic data for RT.[39] Hence, these calculations substantiate the tie lines shown in Fig. 6. A perculiarity of the Cu-In-S system at RT lies in the fact that $CuInS_2$ can coexist in equilibrium with all phases of the entire system except In_2S_3 and $In_{2.8}S_4$. Hence, the present study offers additional prospects for the material development of $CuInS_2$. Experiments in which PAC's are used to control the growth of Cu-In-S thin-film structures are now being performed.

ACKNOWLEDGMENTS

We thank M. L. Fearheily and H. Migge for helpful and stimulating discussions. M. A. Briere is thanked for a critical reading of the manuscript.

[1]S. Wagner and P. M. Bridenbaugh, J. Cryst. Growth **39**, 151 (1977).
[2]J. L. Shay, S. Wagner, and H. M. Kasper Appl. Phys. Lett. **27**, 89 (1975).
[3]H. J. Lewerenz, H. Goslowsky, K.-D. Husemann, and S. Fiechter, Nature **321**, 687 (1986).
[4]K. W. Mitchell, G. A. Pollock, and A. V. Mason, in *Conference Record of the 20th IEEE Photovoltaic Specialist Conference, Las Vegas, 1988,* The Institute of Electrical and Electronics Engineers (Publishing Services IEEE, New York, 1988), Vol. 2.
[5]H. J. Lewerenz *et al.*, J. Mater. Sci. **21**, 4419 (1986).
[6]M. Brüssler, H. Metzner, K.-D. Husemann, and H. J. Lewerenz, Phys. Rev. B **38**, 9268 (1988).
[7]S. C. Abrahams and J. L. Bernstein, J. Chem. Phys. **59**, 5415 (1973).
[8]W. Witthuhn and W. Engel, in *Hyperfine Interactions of Radioactive Nuclei,* edited by J. Christiansen (Springer, Heidelberg, 1983), p. 205.
[9]E. Recknagel, G. Schatz, and Th. Wichert, in *Hyperfine Interactions of Radioactive Nuclei* (Ref. 8), p. 133.
[10]R. Vianden, Hyperfine Interact. **35**, 1079 (1987).
[11]H. Haas and D. A. Shirley, J. Chem. Phys. **58**, 3339 (1973).
[12]J. Bleck, R. Butt, H. Haas, W. Ribbe, and W. Zeitz, Phys. Rev. Lett. **29**, 1371 (1972).
[13]H. Metzner, R. Sielemann, S. Klaumünzer, R. Butt, and W. Semmler, Z. Phys. B **61**, 267 (1985).
[14]*Binary Alloy Phase Diagrams* edited by T. B. Massalski (American Society for Metals, Ohio, 1986).
[15]P. R. Subramanian and D. E. Laughlin, Bull. Alloy Phase Diagrams **10**, 554 (1989).
[16]W. Keppner, T. Klas, W. Körner, R. Wesche, and G. Schatz, Phys. Rev. Lett. **54**, 2371 (1985).
[17]F. Weibke, Z. Metallk. **31**, 228 (1939).
[18]M. Gauneau and R. Graf, C. R. Acad. Sci. Paris, B **266**, 1397 (1968).
[19]R. A. Fournelle and J. B. Clark, Metall. Trans **3**, 2757 (1972).
[20]A. S. Koster, L. R. Wolff, and G. J. Visser, Acta Crystallogr. B **36**, 3094 (1980).
[21]J. W. G. A. Vrolijk and L. R. Wolff, J. Cryst. Growth **48**, 85 (1980).
[22]F. Lawes and H. J. Wallbaum, Z. Angew. Mineral. **4**, 17 (1942).
[23]K. C. Jain, M. Ellner, and K. Schubert, Z. Metallk. **63**, 456 (1972).
[24]T. P. Rajasekharan and K. Schubert, Z. Metallk. **72**, 275 (1981).
[25]V. Simic and Z. Marinkovic, J. Less Common Met. **72**, 133 (1980).
[26]T. Gödecke and K. Schubert, Z. Metallk. **76**, 358 (1985).
[27]M. Frank *et al.*, Z. Naturforsch. Teil A **41**, 104 (1986).
[28]W. J. Duffin and J. H. C. Hogg, Acta Crystallogr. **20**, 566 (1966).
[29]J. H. C. Hogg and W. J. Duffin, Acta Crystallogr. **23**, 111 (1967).
[30]J. J. M. Binsma, L. J. Giling, and J. Bloem, J. Cryst. Growth **50**, 429 (1980).
[31]K. D. Becker and S. Wagner, Phys. Rev. B **27**, 5240 (1983).
[32]Th. Wichert, W. Witthuhn, H. Metzner, and R. Sielemann, in *Submicroscopic Studies of Defects in Semiconductors,* edited by G. Langouche (North-Holland, Amsterdam, in press).
[33]J. L. Shay and J. H. Wernick, *Ternary chalcopyrite semiconductors: growth, electronic properties, and applications* (Pergamon, Oxford, 1975).
[34]J. Flahaut *et al.*, Bull. Soc. Chim., France, **5**, 2382 (1961).
[35]L. Gastaldi and L. Scavamuzza, Acta Crystallogr. B **36**, 2751 (1980).
[36]J. J. M. Binsma, J. Phys. Chem. Solids **44**, 237 (1983).
[37]M. L. Fearheily, N. Dietz, R. Scheer, and H. J. Lewerenz, in *Proceedings of the XIIIth State-of-the-Art Program on Compound Semiconductors, Seattle, 1990,* edited by H. H. Lee *et al.* (Electronics and Dielectric Science and Technology Division, Electrochemical Society, Pennington, New Jersey, 1991).
[38]M. Hansen and K. Anderko, *Constitution of Binary Alloys,* 2nd ed. (McGraw-Hill, New York 1958).
[39]H. Migge, J. Mater. Res. (to be published).